Supplementary materials for: High-level cognition during story listening is reflected in high-order dynamic correlations in neural activity patterns

Lucy L. W. Owen[1], Thomas H. Chang[1,2], and Jeremy R. Manning[1,†]

[1]Department of Psychological and Brain Sciences,
Dartmouth College, Hanover, NH
[2]Amazon.com, Seattle, WA
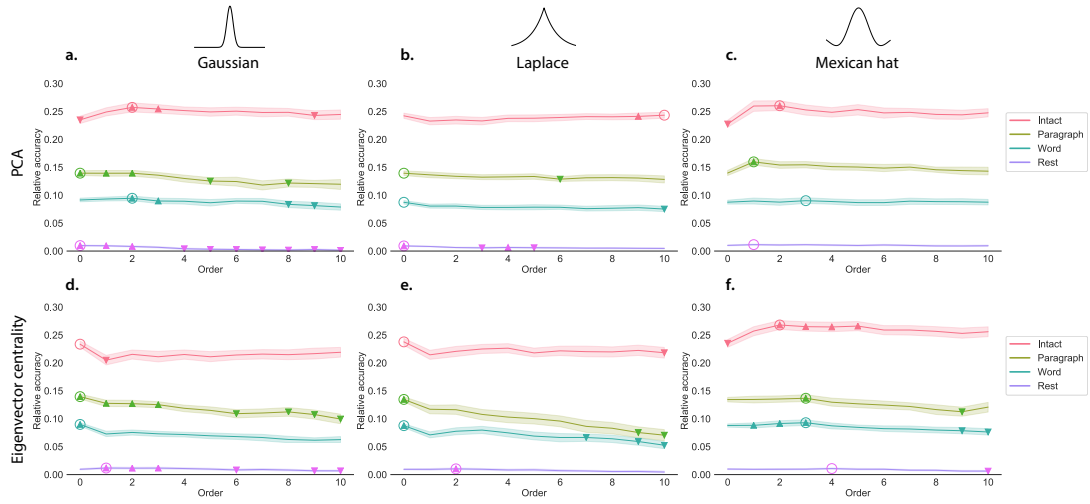[†]Address correspondence to jeremy.r.manning@dartmouth.edu

June 9, 2021

Figure S1: Across-participant timepoint decoding accuracy varies with correlation order and cognitive engagement across kernels. a.-c. Timepoint decoding accuracy as a function of order: PCA. *Order* (*x*-axis) refers to the maximum order of dynamic correlations that were available to the classifiers (see *Feature weighting and testing*). The reported across-participant decoding accuracies for **a. Gaussian**, **b. Laplace**, and **c. Mexican hat** kernel shapes are averaged over all widths (see *Identifying robust decoding results*). The *y*-values are displayed relative to chance accuracy (intact: $\frac{1}{300}$; paragraph: $\frac{1}{272}$; word: $\frac{1}{300}$; rest: $\frac{1}{400}$). The error ribbons denote 95% confidence intervals across cross-validation folds (i.e., random assignments of participants to the training and test sets). The colors denote the experimental condition. Arrows denote sets of features that yielded reliably higher (upward facing) or lower (downward facing) decoding accuracy than the mean of all other features (via a two-tailed *t*-test, thresholded at $p < 0.05$). The circled values represent the maximum decoding accuracy within each experimental condition. Panels a.-c. used PCA to project each high-dimensional pattern of dynamic correlations onto a lower-dimensional space. **d.-f. Timepoint decoding accuracy as a function of order: eigenvector centrality.** These panels are in the same format as Panel a.-c., but here eigenvector centrality has been used to project the high-dimensional patterns of dynamic correlations into lower-dimensional spaces.

2
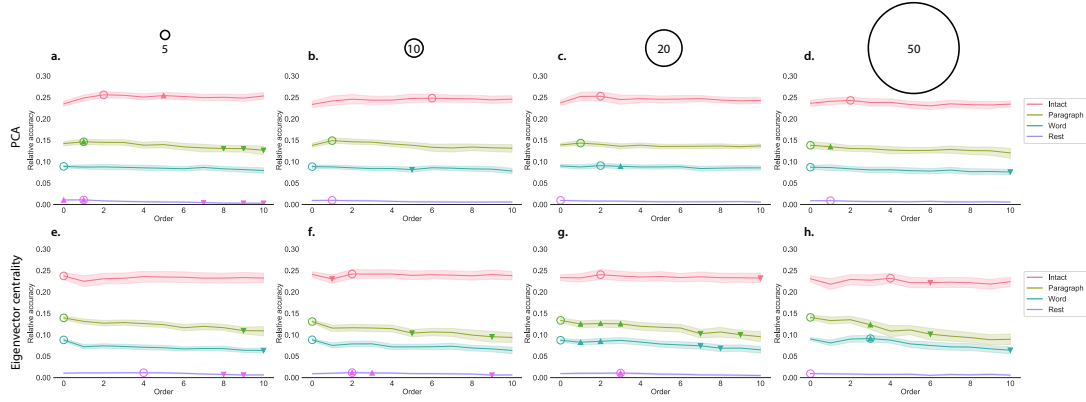
Figure S2: Across-participant timepoint decoding accuracy varies with correlation order and cognitive engagement across widths. a.-d. Timepoint decoding accuracy as a function of order: PCA. *Order* (*x*-axis) refers to the maximum order of dynamic correlations that were available to the classifiers (see *Feature weighting and testing*). The reported across-participant decoding accuracies for kernel widths of **a. 5**, **b. 10**, **c. 20**, and **d. 50** are averaged over all kernel shapes (see *Identifying robust decoding results*). The *y*-values are displayed relative to chance accuracy (intact: $\frac{1}{300}$; paragraph: $\frac{1}{272}$; word: $\frac{1}{300}$; rest: $\frac{1}{400}$). The error ribbons denote 95% confidence intervals across cross-validation folds (i.e., random assignments of participants to the training and test sets). The colors denote the experimental condition. Arrows denote sets of features that yielded reliably higher (upward facing) or lower (downward facing) decoding accuracy than the mean of all other features (via a two-tailed *t*-test, thresholded at $p < 0.05$). The circled values represent the maximum decoding accuracy within each experimental condition. Panels a.-d. used PCA to project each high-dimensional pattern of dynamic correlations onto a lower-dimensional space.**e.-h. Timepoint decoding accuracy as a function of order: eigenvector centrality.** These panels are in the same format as Panel a.-d., but here eigenvector centrality has been used to project the high-dimensional patterns of dynamic correlations into lower-dimensional spaces.

3
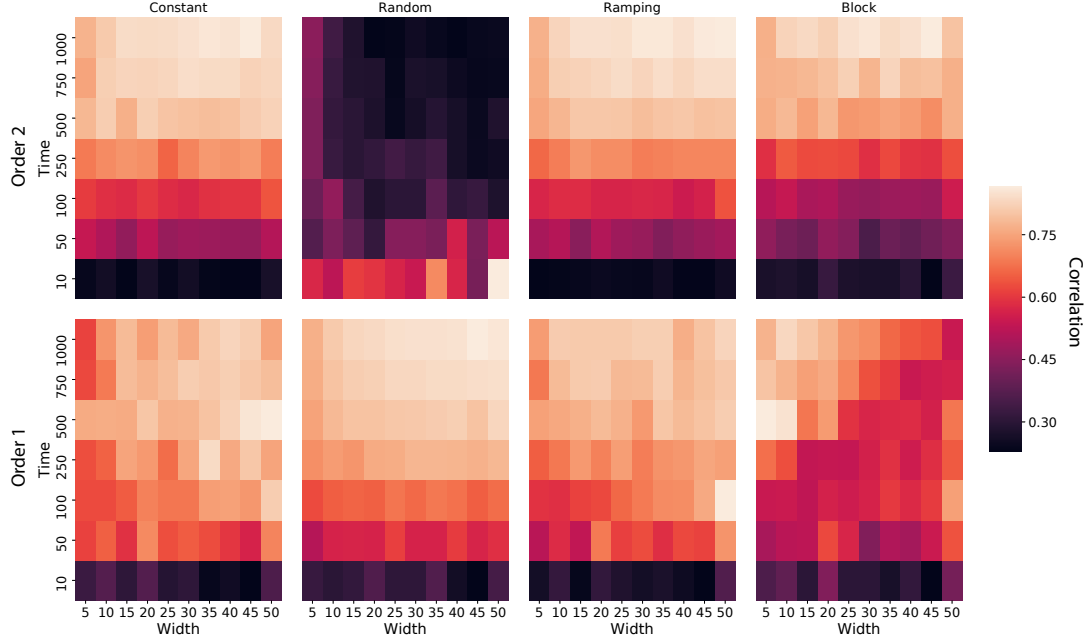
Figure S3: Recovery heatmap of simulated first-order and second-order dynamic correlations across time and widths. Each panel displays a heatmap of the average correlations between the vectorized upper triangles of the recovered first-order and second-order correlation matrices and the true (simulated) first-order and second order correlation matrices. The averages are taken across several randomly generated synthetic datasets for each timeseries pattern (constant, random, ramping, and data; see *Synthetic data: simulating dynamic higher-order correlations*). The *x*-axes of each heatmap denote varying Laplace-shaped kernel widths (see Figs. S1 and S2), and the *y*-axes of each heatmap denote varying durations (in samples) of the synthetic datasets. A total of 10 synthetic datasets were generated for each duration (row) and timeseries pattern (panel).
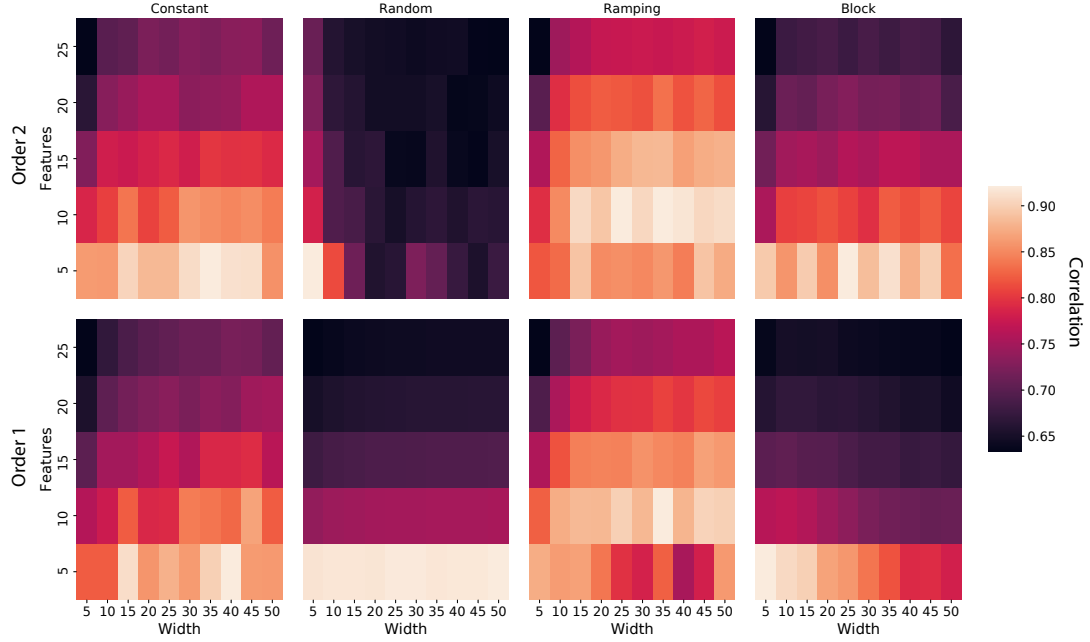
Figure S4: Recovery heatmap of simulated first-order and second-order dynamic correlations across features and widths. Each panel displays a heatmap of the average correlations between the vectorized upper triangles of the recovered first-order and second-order correlation matrices and the true (simulated) first-order and second order correlation matrices. The averages are taken across several randomly generated synthetic datasets for each timeseries pattern (constant, random, ramping, and data; see *Synthetic data: simulating dynamic higher-order correlations*). The *x*-axes of each heatmap denote varying Laplace-shaped kernel widths (see Figs. S1 and S2), and the *y*-axes of each heatmap denote varying numbers of features (*K*) used in each of the synthetic datasets. A total of 10 synthetic datasets were generated for each number of features (row) and timeseries pattern (panel).

Figure S5: Top terms associated with the most strongly correlated nodes at each order, for the *intact* experimental condition. Each color corresponds to one order of inter-subject functional correlations. The inflated brain plots display the locations of the endpoints of the 10 strongest (absolute value) correlations at each order, projected onto the cortical surface (Combrisson et al., 2019). The lists of terms display the top 10 Neurosynth terms (Rubin et al., 2017) decoded from the corresponding brain maps for each order. (Also see Fig. 6, top row, in the main text.)

Order
0   5   10   15

Order 1	Order 2	Order 3	Order 4	Order 5
sounds	voice	auditory cortex	gyri	occipital
auditory cortex	precuneus	sound	temporo	extrastriate
listening	temporal	sounds	posterior temporal	visual
auditory	speaker	auditory	posterior middle	reaching
listened	temporal gyrus	heschl gyrus	temporo parietal	objects
auditory stimuli	spoken	heschl	visual stream	arm
speech	heard	acoustic	secondary somatosensory	dlpfc
primary auditory	sounds	gyrus stg	insular	incorrect
sound	comprehension	planum	verb	occipital gyrus
acoustic	speech perception	listened	temporal gyri	index finger

Order 6	Order 7	Order 8	Order 9	Order 10
anterior temporal	fusiform	ventrolateral	chinese	prefrontal
mental states	object	fusiform gyrus	reading	prefrontal cortex
lateral temporal	memory encoding	inferior frontal	naming	dorsolateral prefrontal
tom	fusiform gyrus	inferior	judgment	cortex precuneus
pole	fusiform gyrus	fusiform	letter	precuneus posterior
temporal pole	venral visual	intentions	english	medial
comprehension	faces	pfc	speakers	dorsolateral
virtual	reaching	cognitive impairment	outcomes	precuneus
mind tom	parahippocampal gyrus	semantic	ventral striatum	dorsomedial prefrontal
theory of mind	objects	mild cognitive	nucleus accumbens	medial prefrontal

Order 11	Order 12	Order 13	Order 14	Order 15
tactile	ifg	inferior parietal	musical	tom
secondary somatosensory	gyrus ifg	parietal lobule	anterior superior	mind tom
precuneus	viewing	working memory	superior temporal	temporal
somatosensory cortex	angular gyrus	ipl	listening	medial
pain	v5	working	spoken	temporal sulcus
temporo parietal	angular	anterior intraparietal	music	dorsomedial prefrontal
primary somatosensory	motion	parietal cortex	comprehension	theory mind
somatosensory	social interaction	frontoparietal	voice	sts
somatosensory cortices	visual	fronto parietal	speech	dorsomedial
precuneus posterior	temporo parietal	posterior parietal	frontal operculum	medial prefrontal

Figure S6: Top terms associated with the most strongly correlated nodes at each order, for the *paragraph* experimental condition. This figure is in the same format as Figure S5, but displays results for the paragraph-scrambled story listening condition. (Also see Fig. 6, second row, in the main text.)

Order 1

listening
speech
voive
sounds
speeck perception
spoiken
listened
audiory
superior temporal
temporal gyrus

Order 2

voice
temporal gyrus
sounds
listening
speech
spoken
audisotry
superior temporal
listened
speech perception

Order 3

temporal gyrus
voice
superior temporal
temporal sulcus
speaker
sts
speech
listening
spoken
superior

Order 4

anterior temporal
expression
lateral temporal
temporal lobes
lobes
temporal lobe
fearful faces
temporal
lobe
neutral faces

Order 5

mild cognitive
memory
medial temporal
lobe
mtl
retrieval
episodic
temporal lobe
lobe mtl
episodic memory

Order 6

inferior parietal
default mode
default
inhibition
pcc
posterior cingulate
response inhibition
medial
autobiographical
dmn

Order 7

anterior temporal
amygdala insula
expression
amygdala
anterior prefrontal
neutral faces
temporal lobbe
anxiety
fearful faces
amygdala responses

Order 8

parahippocampal
episodic
parahippocampal gyrus
hippocampus
hippocampal
memory
medial temporal
anterior hippocampus
episodic memory
temporal lobe

Order 9

face
fusiform face
face ffa
ffa
fusiform
faces
fusiform gyrus
reaching
occipital
face recognition

Order 10

extrastriate
occipitotemporal cortex
occipitotemporal
videos
v5
visual
mt
perception
fusiform
objects

Order 11

primary somatosensory
premotor
anterior temporal
somatosensory
premotor cortex
inferior parietal
s1
ventral premotor
execution
somatosensory cortex

Order 12

medial prefrontal
medial
anterior temporal
prefrontal cortex
prefrontal
semantic memory
negative positive
mpfc
autobiographical
temporal lobe

Order 13

reaching
retrosplenial
visuomotor
tools
precuneus
videos
touch
cortex precuneus
navigation
retrosplenial cortex

Order 14

locations
precuneus
body
supramarginal
videos
actions
mt
video clips
video
occipitotemporal

Order 15

medial
posterior cingulate
pcc
medial prefrontal
cortex precuneus
referential
self referential
cortex posterior
autobiographical
hippocampus

Figure S7: Top terms associated with the most strongly correlated nodes at each order, for the *word* experimental condition. This figure is in the same format as Figure S5, but displays results for the word-scrambled story listening condition. (Also see Fig. 6, third row, in the main text.)

Order 1

cortex parietal
intraparietal
parietal cortex
ips
posterior parietal
parietal
intraparietal sulcus
symbbolic
superior parietal
prefrontal parietal

Order 2

occipital
visual
etrastriate
vision
occipital cortex
visual cortex
visual stream
motion
v1
mt

Order 3

parietal
conflict
task
visual cortex
working memory
supplementary motor
working
arithmetic
supplementary
anterior temporal

Order 4

default
autobiographical
default mode
posterior cingulate
anterior temporal
dmn
early visual
mental imagery
primary visual
autobiographical memory

Order 5

dorsolateral
frontal
middle frontal
motion
mt
verbal
memory
visual motion
dorsolateral prefrontal
vision

Order 6

locations
navigation
medial
medial prefrontal
orienting
precuneus
memory retrieval
location
retrieval
dorsomedial

Order 7

insual anterior
error
anterior insula
monitoring
insula
conflict
frontal cortex
insular
taste
errors

Order 8

occipital
precuneus
letter
inferior occipital
visual
cortex precuneus
occipital cortex
lateral occipital
spatially
sulcus

Order 9

posterior insula
temporal lobe
mtl
amygdala responses
lobe mtl
insula
lobe
mild cognitive
insular
cognitive impairment

Order 10

inferior occipital
anterior prefrontal
face
selective
face ffa
dlpfc
ffa
fusiform face
dorsolateral
cortex dlpfc

Order 11

hippocampal
hippocampus
anterior hippocampus
lobe
amygdala hippocampus
parahippocampal gyrus
mtl
medial temporal
temporal lobe
lobe mtl

Order 12

food
ofc
cortex ofc
orbitofrontal cortex
nucleus accumbens
accumbes
orbitofrontal
value
orbital
hypothalamus

Order 13

insula
taste
insular
insular cortex
unpleasant
pleasant
amygdala
amygdala insula
posterior insula
pain

Order 14

amygdala hippocampus
hippocampal
hippocampus
anterior hippocampus
medial temporal
amygdala
parahippocampal
navigation
unpleasant
episodic

Order 15

s1
striatal
outcomes
monetary
memory encoding
accumbens
mesolimbic
nucleus accumbens
frontal
money

Figure S8: Top terms associated with the most strongly correlated nodes at each order, for the *rest* experimental condition. This figure is in the same format as Figure S5, but displays results for the resting state condition. (Also see Fig. 6, bottom row, in the main text.)
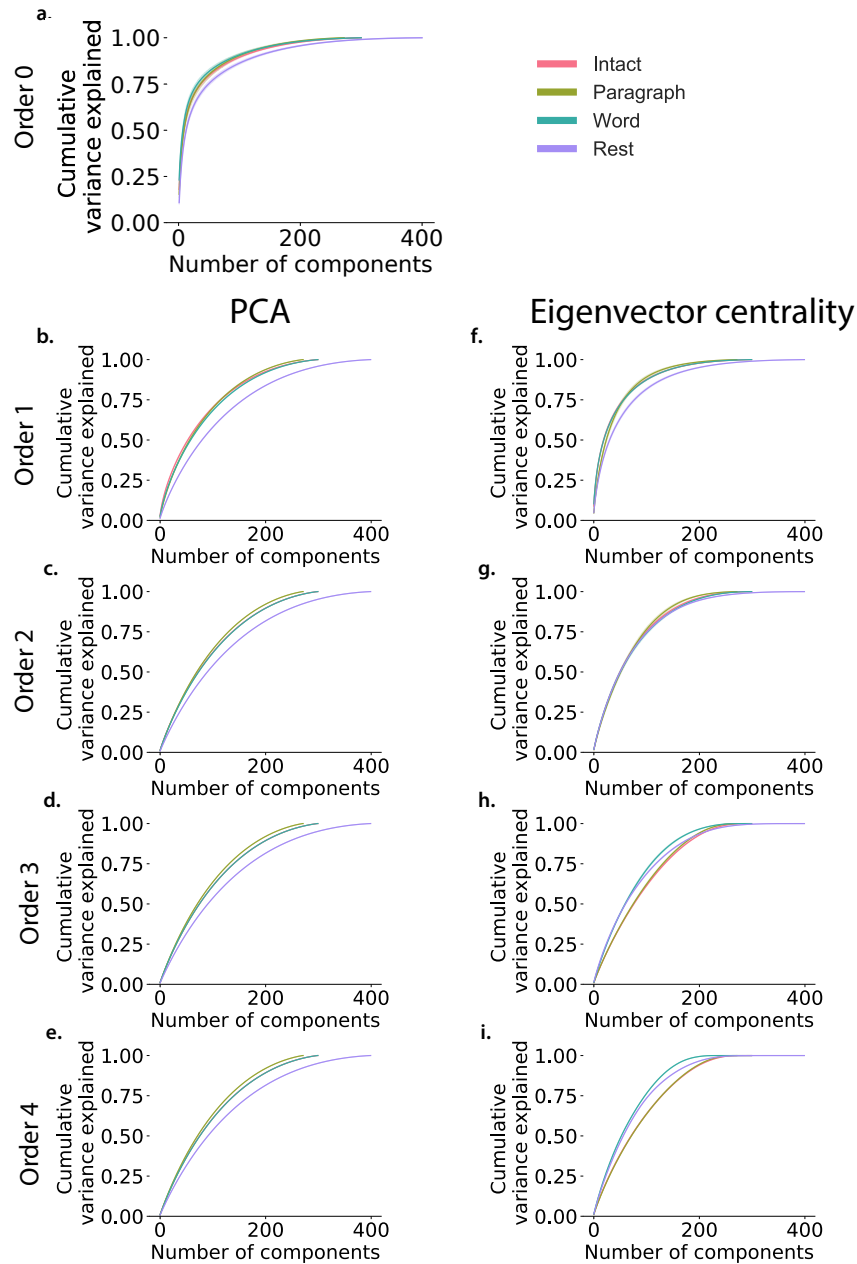
Figure S9: Cumulative percent variance explained as a function of the number of principle components. *Order* refers to the order of the dynamic correlations calculated. Principle components analysis was performed, and reduced independently for each subject. Maximum number of components varies with the total time for each condition (intact: 300; paragraph: 272; word: 300; rest: 400). **a. Cumulative percent variance as a function of number of components for Order 0.** PCA was performed on the raw activity patterns (Order 0). **b.-e. Cumlative percent variance as a function of number of components for Orders 1.-4.: PCA** Dynamic correlation were calculated for orders 1-4 using PCA to project each high-dimensional pattern of dynamic correlations onto a lower-dimensional space. **f.-i. Cumlative percent variance as a function of number of components for Orders 1.-4.: eigenvector centrality.** These panels are in the same format as Panel b.-e., but here eigenvector centrality has been used to project the high-dimensional patterns of dynamic correlations onto a lower-dimensional space.

Supplementary references

Combrisson, E., Vallat, R., O'Reilly, C., Jas, M., Pascarella, A., l Saive, A., Thiery, T., Meunier, D., Altukhov, D., Lajnef, T., Ruby, P., Guillot, A., and Jerbi, K. (2019). Visbrain: a multi-purpose GPU-accelerated open-source suite for multimodal brain data visualization. *Frontiers in Neuroinformatics*, 13(14):1–14.

Rubin, T. N., Kyoejo, O., Gorgolewski, K. J., Jones, M. N., Poldrack, R. A., and Yarkoni, T. (2017). Decoding brain activity using a large-scale probabilistic functional-anatomical atlas of human cognition. *PLoS Computational Biology*, 13(10):e1005649.